



ORIGINAL ARTICLE

Synthesis, physicochemical characterization, antifungal activity and toxicological features of cerium oxide nanoparticles



Isabela A.P. Farias^{a,*}, Carlos C.L. Santos^a, Aline L. Xavier^a, Tatianne M. Batista^a, Yuri M. Nascimento^a, Jocianelle M.F.F. Nunes^a, Patrícia M.F. Silva^b, Raimundo A. Menezes-Júnior^a, Jailson M. Ferreira^c, Edeltrudes O. Lima^a, Josean F. Tavares^a, Marianna V. Sobral^a, Dawy Keyson^a, Fábio C. Sampaio^a

^a Federal University of Paraíba, Campus I, João Pessoa, PB, Brazil

^b State University of Paraíba, Campina Grande, PB, Brazil

^c Federal Institute of Education, Science and Technology of Paraíba, João Pessoa, PB, Brazil

Received 2 June 2020; accepted 25 October 2020

Available online 4 November 2020

KEYWORDS

Candida albicans;
Antifungal activity;
Toxicity;
Nanoparticles;
Cerium oxide;
Inhibitory concentration

Abstract Fungal infection is a public health problem. Antifungal agents resistance is often seen in common *Candida albicans* in the hospital environment. Nanoparticles have been reported in the literature as a promising development of health products. The toxicity, antioxidant and antifungal activity of cerium oxide nanoparticles (CeNP) were evaluated. After synthesis and characterization of the physicochemical properties, the new CeNP was evaluated by biological tests of antifungal activity. The antioxidant activity of CeNP was evaluated by scavenging free radicals of 1,1-diphenyl-2-picrylhydrazyl hydrate (DPPH). The DPPH scavenging activity was monitored by % color inhibition the absorbance. *In vivo* acute toxicity studies of CeNP were carried out by oral administration in mice (300 and 2000 mg/kg, n = 3/ group), and by brine shrimp (*Artemia salina*) model (0.001-25 mg/ mL, n = 10/ group). CeNP was able to interfere in the fungal growth, depending on the strain and dosage used. Acute lethal dose 50% is greater than 2000 mg/kg and CeNP did not induce toxicity for *A. salina*. Antioxidant activity was not significant. The current antifungal

* Corresponding author at: Federal University of Paraíba, Campus Universitário I, Cidade Universitária, CEP: 58059-900, João Pessoa, PB, Brazil.

E-mail address: isabela.passos@academico.ufpb.br (I.A.P. Farias).

Peer review under responsibility of King Saud University.



Production and hosting by Elsevier

and toxicity features results support the use of CeNP as antifungal agent against *Candida albicans* strains, which may find applications in biotechnology and biomedical area in the development of a new nano-biomaterial for clinical applications.

© 2020 The Authors. Published by Elsevier B.V. on behalf of King Saud University. This is an open access article under the CC BY-NC-ND license (<http://creativecommons.org/licenses/by-nc-nd/4.0/>).

1. Introduction

Fungal infections represent a public health problem. *Candida albicans* is the most commonly involved species in hospital infections. This dimorphic yeast is commensal and colonizes the blood, skin, the gastrointestinal, and the reproductive tracts. Occurrences are growing together with the increase of immunocompromised and hospitalized patients worldwide (Mohr et al., 2020; Koehler et al., 2019; Zhan et al., 2015; Lim et al., 2012).

Antifungal agents for treatment or prophylaxis of invasive fungal infections are limited to four classes: azoles, echinocandins, polyenes, and flucytosine. Currently, antifungal oral administration schemes include oral or intravenous. In case of oropharyngeal candidiasis, nystatin oral suspension or oral fluconazole are indicated (Pappas et al., 2016).

The often long duration of treatments, or the high frequency use of these agents for prophylactic purposes facilitates the emergence of isolated resistance, whether by previously susceptible strains that acquire resistance, or by new species that are naturally resistant (Fekkar et al., 2014). Resistance to fluconazole, voriconazole, and itraconazole is often seen in common *Candida* species in the hospital environment (Zhan et al., 2015).

In general, the CeO₂-based materials are used in well-established applications on industrial (catalyst of soot combustion in the automotive three way catalysts), prototypes and niche applications (solid oxide fuel cells, and polymer exchange membrane Fuel Cells), and emerging applications (reforming of hydrocarbons or oxygenated; water-gas shift reaction and preferential oxidation of CO; oxidation of volatile organic compound; dehalogenation; partial hydrogenation; photocatalysis; thermochemical water splitting, organic reactions, and biomedical applications) (Montini et al., 2016).

Upon decrease of the particle size, distinct physical and chemical properties as compared to bulk materials arise including increase mobility of oxygen and versatile and superior active catalytic support for energy processes. Cerium oxide nanoparticles (CeNP) have been applied in catalyst systems, as metal catalyst combined with another metal species that acts as the active species; in energy applications (H₂ production/purification, fuel cells and photocatalytic water splitting) (Melchionna and Fornasiero, 2014); and biological activity as anti-inflammatory (Hirst et al., 2009), antimicrobial (Farias et al., 2018), radioprotective effects on stem cells (Salveti et al., 2020), potential pharmaceutical approach for the treatment of neurodegenerative diseases (Battaglini et al., 2019) and of obesity (Rocca et al., 2015).

The surface valence state (Ce⁴⁺ and/or Ce³⁺) is important in CeNP effect and biological applications (Zeyons et al., 2009). Studies show that CeNP exhibit anti-inflammatory action, antioxidant properties, ability to stimulate proliferation and migration of fibroblasts, keratinocytes, and vascular

endothelial cells. The nanoparticles may be useful as a novel therapy for acute and chronic inflammation (Chigurupati et al., 2013; Hirst et al., 2009), including in topical system of application whereas CeNP has capacity to permeation of dermal and transdermal intact and damaged human skin after prolonged exposure (Mauro et al., 2019).

Antimicrobial activity of CeNP has been observed against *Bacillus subtilis* (Babu et al., 2014; Krishnamoorthy et al., 2014; Pelletier et al., 2010), *Enterococcus faecalis* (Krishnamoorthy et al., 2014), *Escherichia coli* (Babu et al., 2014; Krishnamoorthy et al., 2014; Babenko et al., 2012; Pelletier et al., 2010; Zeyons et al., 2009), *Salmonella enteritidis* (Babu et al., 2014), *Salmonella typhimurium* (Krishnamoorthy et al., 2014), *Staphylococcus aureus* (Babu et al., 2014; Babenko et al., 2012), *Synechocystis* (Zeyons et al., 2009), and *C. albicans* (Babenko et al., 2012; Pujar et al., 2020). In general, antimicrobial activity of CeNP on opportunistic microorganisms was extensively reviewed (Farias et al., 2018).

The surface valence state of particles influences the protective or antimicrobial effect of nanoparticle. Conversion of Ce⁴⁺ to Ce³⁺ was observed in *Escherichia coli* (Zeyons et al., 2009).

The ability to scavenge free radicals of the CeNP was observed in studies with J774A.1 murine macrophage cells (Hirst et al., 2009); and with hippocampus and cerebellum (Hardas et al., 2012).

In the biological context, the effect of these nanotechnologies has not been accompanied by exhaustive toxicological studies designed (Mauro et al., 2019). Thus, to obtain significant results in acute toxicity tests, investigation of different biological models with vertebrates (mice) and invertebrates (*Artemia salina*) is proposed. Brine shrimp (*A. salina*) is a zooplankton used in feed for fish, and is considered an adequate toxicology model for nanomaterials (Ozkan et al., 2016; Rajabi et al., 2015; Gambardella et al., 2014). *A. salina* is included as a test species by the United States Environmental Protection Agency for acute toxicity testing (EPA, 2002). The acute toxicity test in rodents is the principal *in vivo* test for the evaluation of safety profile of a substance (Parasuraman, 2011). There is an imminent need to monitor existing antifungals and *Candida* susceptibility at national and international levels (Zhan et al., 2015); production of antifungal agents is also an imperative.

The aims of this study were to evaluate the acute toxicity of CeNP on vertebrates (mice) and invertebrates (*A. salina*) and to investigate its antifungal and antioxidant activity.

2. Material and methods

2.1. Reagents and chemicals

CeNPs were synthesized in the Chemistry Laboratory, at the Federal University of Paraiba, Brasil. Cerium (IV) sulfate (p. a., purity ≥ 98%) and sodium hydroxide (Vetec™ reagent

grade, purity $\geq 97\%$) were purchased from Sigma-Aldrich (Merck, Merck KGaA, Darmstadt, Germany). All chemicals used were of analytical grade and used as received without further purification. Dimethylsulfoxide was purchased from Mallinckrodt Chemicals® (Phillipsburg, NJ, USA). Sodium thiopental (Thiopentax®) was purchased from Cristália (Itapira, SP, Brazil), and heparin (Parinex®) from Hipolabor (Sabará, MG, Brazil). Kits for biochemical and hematological analysis were purchased from LABTEST® (Lagoa Santa, MG, Brazil). Sabouraud dextrose broth and agar were purchased from HiMedia, India. LIVE/DEAD BacLight™ Viability Kit was purchased from Invitrogen™ (Molecular Probes Inc., OR, USA). Universal pH-indicator strips were purchased from Merck Quimical, São Paulo, Brazil. All other reagents were purchased from Sigma-Aldrich (St. Louis, MO, USA).

2.2. Synthesis and characterization of cerium oxide nanoparticles

The synthesis of CeNP was performed by the microwave hydrothermal method (Soren et al., 2015), starting from 0.5 mmol of cerium (IV) sulfate in 100 ml of distilled water. Then, 5 mol/L NaOH solution was added drop wise under mild stirring until the pH of solution becomes 14. The reaction system was heated and treated in microwave at 150 °C for 5 min.

The material (after drying) was referred for characterization where its structural properties (Khan et al., 2019) were evaluated by X-ray diffraction (XRD); Stephen Brunauer, Paul Hugh Emmett and Edward Teller (BET) method (Brunauer et al., 1938; density of 7.2 g/cm³ for the cerium oxide sample), high resolution scanning electron microscopy (SEM), transmission electron microscopy (TEM) and X-ray energy dispersion analysis spectroscopy (EDS). The optical properties of CeNP was evaluate using spectra in the UV-Vis in the range of wavelengths between 190 and 900 nm.

The average CeNP crystallite size (P_{BET}) was also calculated using the following formula (Eq. (1); Raghupathi et al., 2011).

$$P_{BET} = 6/\rho_t \cdot \alpha_{sBET} \quad (1)$$

where ρ_t is theoretical density of CeO₂ (7.2 g/cm³), and α_{sBET} is the BET surface area (295 m²/g).

The average crystallite of the sample too was calculated by using the Debye-Scherrer formula (Eq. (2)):

$$Dp = 0.9 \cdot \lambda/\beta \cdot \cos\theta \quad (2)$$

where Dp is the average crystallite size, λ is the wavelength of the CuK α line, θ is the Bragg angle, and β is the Full Width at Half-Maximum (FWHM) of the diffraction peak in radians. The lattice parameter of cerium oxide nanoparticles was measured using x-ray diffraction XRD.

The zeta potential was measured using a Zetatrac instrument (Microtrac, USA). The CeNPs were resuspended in distilled-deionized water (pH 7.2). The analysis was performed in triplicate. Measurements were essentially as described elsewhere (Pelletier et al., 2010).

2.3. Minimum inhibitory concentration and minimum fungicidal concentration

In order to investigate the minimum inhibitory concentration (MIC) and minimum fungicidal concentration (MFC) of

CeNPs, the following *C. albicans* clinical (LM), and American Type Culture Collection (ATCC) strains were used: ATCC 1106, ATCC 76485, ATCC 76645, ATCC 60193, ATCC 26645, LM 62, LM 92, LM 157, LM 38, LM 227 and LM 65 ($1-5 \times 10^6$ UFC/mL). They were cultivated on Sabouraud Dextrose Broth (SDB).

CeNP resuspended in DMSO (dimethylsulfoxide) was prepared in concentrations of 150 mg/mL, along with a positive control (Miconazole Nitrate). The concentration of DMSO did not exceed 0.4% in the assays.

MIC of the suspension was assessed by microdilution method. Six rows of wells were prepared with final concentrations from 0.01 to 75 mg/mL for CeNP, and from 5 to 400 μ g/mL for Miconazole Nitrate. All three remaining rows of wells were filled with the oxidation-reduction indicator resazurin.

Subsequently, the concentration corresponding to the minimum inhibitory and the two concentrations immediately more concentrated were cultivated on Sabouraud dextrose agar plates. MFC was determined as the lowest concentration showing no visible colony formation after incubation for 24 h at 37 °C.

2.4. Growth kinetic study

Three *C. albicans* strains (ATCC 1106, ATCC 76485 and LM 38) were selected for viability in experimental fluorescence assays (Jin et al., 2005). In summary, the fluorescence assay distinguishes between live and dead fungi. A standard curve was constructed using different proportions of viable (green fluorescence) and non-viable (red fluorescence) fungi cells. The curve was constructed with concentrations of 0, 20, 50, 80, and 100% live fungi using the LIVE/DEAD BacLight™ Viability Kit. A standardized concentration of 0.5 McFarland scale (10^6 CFU/mL) from the fungi cells was prepared with saline solution. The growth of the fungal strain was evaluated at 1, 4, 8, and 10 h; and measured for optical density at 600 nm by spectrophotometer (Fluostar Optima - BMG Labtech, Germany). The tests were carried out in triplicate and repeated three times on different days.

2.5. Analysis of the substrate pH

A special care was dedicated to measure the influence of the interaction between nanoparticles and microorganisms studied on the pH of cultivation medium. Then, biotic and abiotic environment was established. Evaluation of change in the pH of the medium on CeNP contact with *C. albicans* was performed with universal pH 0-14 tape. The ATCC 60193 strain was randomly selected, grown in SDB for 48 h at 37° C and standardized ($1-5 \times 10^6$ CFU/mL). The CeNP suspension 5 mg/mL received more SDB and fungal inoculum suspension to obtain a final 3.17 mg/mL (MIC selected strain) in 100 μ L. Controls were SDB + fungi and SDB + CeNP suspension at 3.17 mg/mL. The test was performed in quadruplicate on three different days.

2.6. DPPH radical scavenging activity

The free radical scavenging capacities of the CeNP were tested by their ability to bleach the stable 1,1-diphenyl-2-picrylhydrazyl hydrate (DPPH) radical. The reaction mixture

contained 30 μM DPPH and different concentrations of CeNP (1, 5, 10, 15, 20 $\mu\text{g}/\text{mL}$) in 1 ml methanol. After 90 min of incubation at room temperature, the radical scavenging potential of the antioxidant was measured by % color inhibition the absorbance was taken at 517 nm (Soren et al., 2015). The inhibition rate of the DPPH free radical was calculated as follows (Eq. (3)):

$$\% \text{ Inhibition } \left\{ \left[\frac{\text{Absorbance}_{\text{negative control}} - (\text{Absorbance}_{\text{sample}} - \text{Absorbance}_{\text{Blank}})}{\text{Absorbance}_{\text{negative control}}} \right] \times 100 \right\} \quad (3)$$

Ascorbic acid was used as standard. The tests were carried out in triplicate and repeated three times on different days.

2.7. Animals, housing, diet, and water

The animals were obtained from the Dr. Thomas George Bacterium (Research Institute in Drugs and Medicines/Federal University of Paraíba, Brazil). In the acute oral toxicity study, 8–12 weeks old Swiss female mice (*Mus musculus*), in the weight range from 28.0 to 32.0 g on the first day of treatment, were acclimatized for 7 days before initiation of dosing.

Animals were housed in standard polypropylene cages with a controlled 12 h light/dark cycle. Temperature was maintained at 19–25 $^{\circ}\text{C}$ with a relative humidity of 30–55%. Potable water and standardized diet were provided ad libitum.

Experimental protocols and procedures were approved by the local animal ethics committee (protocol number 016/2016) which follows the international principles in ethics for animal experimentation.

2.8. Experimental design-acute toxicity on mice

The acute oral toxicity of CeNP was assessed in accordance with the Organization for Economic Cooperation and Development (OECD) guideline 423 (OECD, 2001). Briefly, CeNP (300 mg/kg) was administered orally in a single dose by gavage to three mice. After 14 days of observation, and accounting of the number of live and dead animals, three animals were dosed sequentially with the same dose. The study continued by testing two more groups of three animals with 2000 mg/kg of CeNP.

CeNP was resuspended in 5% (v/v) Tween-80 in saline. For each assay with a dose of CeNP, a group control ($n = 3$) administered with vehicle alone (5% (v/v) Tween 80 in saline) was used. After the administration of CeNP, the animals were reviewed cage-side for signs of toxicity, morbidity and mortality at the following time points: 15 min, 30 min, 1 h, 4 h and once a day for 14 days. Histopathological examination was performed for all living mice on day 15. Mice were observed for behavioral changes related to central nervous system (stimulant and depressant activity) and autonomic nervous system, among other abnormal behaviors (Almeida et al., 1999). Food and water consumption were measured daily and body weight of each mouse was taken at the initiation and the end of treatment (day 14).

At the end of the study, blood samples for hematology and biochemistry evaluation were collected from the retroorbital

plexus under light anesthesia induced by sodium thiopental intraperitoneal administration (40 mg/kg) and heparin was used as an anticoagulant. Food was withheld for approximately 4 h before blood collection. Hematological examinations were performed using an automatic hematology analyzer, Animal Blood Counter Vet (Horiba ABX Diagnostics) for the following parameters: white blood cell count (WBC), red blood cell count (RBC), hemoglobin concentration (HGB), hematocrit value (HCT), mean corpuscular volume (MCV), mean corpuscular hemoglobin (MCH), mean corpuscular hemoglobin concentration (MCHC). Differential leukocytes count was obtained with an optical microscope for the following parameters: lymphocytes, neutrophils, monocytes, eosinophils and basophils. Serum biochemistry was performed using a spectrophotometer Cobas Mira Plus® (Roche Diagnostic System, Livingston, UK) for the following parameters: alanine aminotransferase (ALT), aspartate aminotransferase (AST), urea and creatinine.

All animals were subjected to necropsy, and heart, liver, kidney, spleen and thymus were excised, weighed to determination of indexes of organs [organ weight (mg)/body weight(g)] and then preserved in neutral buffered 10% formalin. Liver and kidney samples were submitted to microscopic examination. Portions of these organs were cut into small pieces (5 μm), followed by staining of the histological sections with hematoxylin-eosin and masson for liver. Histological analysis was performed by light microscopy to determine the presence and extent of liver or kidney lesions attributed to the CeNP. Systems of scores to grade liver and kidneys lesions were employed as previously described (Medeiros et al., 2010; Brunt et al., 1999).

2.9. Experimental design-acute toxicity on *Artemia salina*

A 25 cm long, 25 cm wide, and 25 cm high, glass aquarium, illuminated with LED lamp was used for hatching the cysts of *A. salina* (Linnaeus, 1758; Anostraca, Brachiopoda, Crustacea) in artificial seawater (3%, m/v) (Ozkan et al., 2016). The temperature was kept constant at 20 $^{\circ}\text{C}$, and the pH between 7.0 and 8.0.

The toxicity test was carried out at different concentrations of CeNP 0.001, 0.01, 0.1, 1.0, 5.0, 10.0, 15.0, 20.0 and 25 mg/mL. After 48 h, the number of dead nauplii were counted as previously described (Ozkan et al., 2016; Gambardella et al., 2014). All of the tests were performed in quadruplicate on different days.

2.10. Statistical analysis

The data collected were submitted to descriptive and inferential statistical analysis using the SPSS (Statistical Package for the Social Sciences) version 20.0 (SPSS Inc., Chicago, IL, USA). In general, data are presented as mean and standard deviation. For mice toxicity data mean \pm standard error was used. Student *t* test was used to compare the means of the inhibition zones, and the ANOVA with Tukey post-test to distinguish between average absorbance differences and toxicity profile. Results were considered significant when $p < 0.05$.

3. Results

3.1. Synthesis and characterization of cerium oxide nanoparticles

Through the BET analysis, it was determined that the CeNP sample synthesized by hydrothermal microwave method had a specific surface area of about 295 m²/g.

The SEM (Fig. 1A), reveals various particle sizes, presenting both linear structures, and thin (nm) overlapping layers.

The average crystallite size values were also determined by TEM investigation (Additional file 1). The size is determined by counting 100 particles. The mean \pm SD size distribution of CeNP was 4.10 \pm 0.99 nm diameter. The panoramic TEM image (Fig. 1B) shows nanoparticles.

The average calculated particle size by P_{BET} was found to be 3–5 nm. The average crystallite size calculated by the

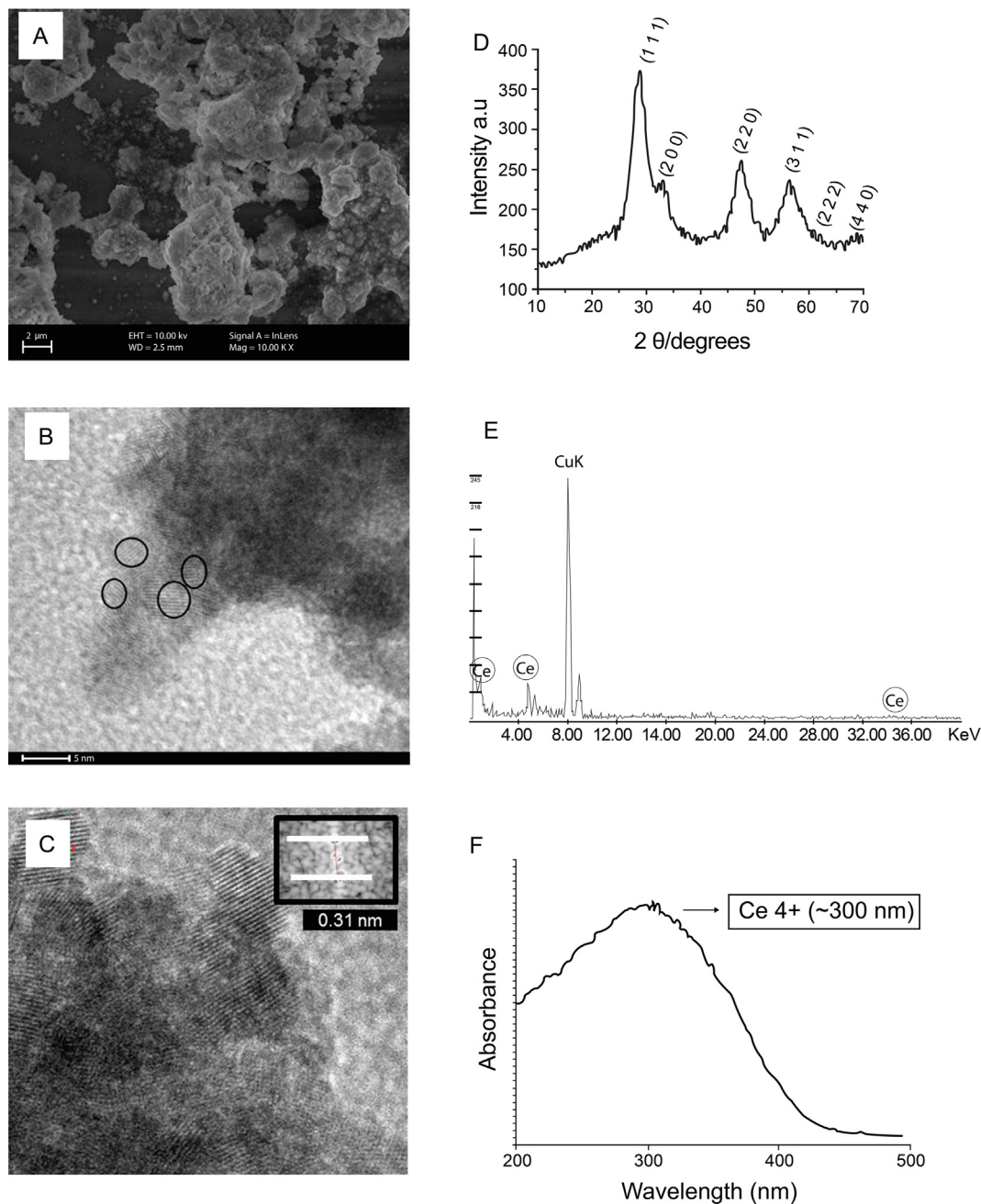


Fig. 1 Characterization of CeNP. (A) Scanning Electron Microscopy image: the general status of CeNP nanoparticles confirming the presence of nanocrystallites in agglomerates. (B) Transmission electron microscopy (TEM) panoramic image of CeNP with uniform size and rounded shapes of about 4 nm. (C) TEM reveals interplanar spacings in agreement with the CeNP structure; (D) X-ray diffraction pattern of CeNP exhibited six typical peaks corresponding to (1 1 1), (2 0 0), (2 2 0), (3 1 1), (2 2 2), (4 0 0) planes, which are typical of cubic fluorite structure of CeNP; (E) Typical X-ray energy dispersive spectroscopy (EDS) spectra of CeNP taken during TEM. (F) UV – VIS absorption spectra of CeNPs with maximum absorption at 300 nm, indicative of their higher Ce⁴⁺ content.

Debye-Scherrer formula was about 3.17 nm. These average particle sizes calculated reported are consistent with the TEM study. The TEM picture shown in Fig. 1B the strong agglomeration of small particles with a diameter on the order of about 4 nm, and interplanar distances of about 0.31 nm (Fig. 1C).

The cubic fluorite structure of cerium oxide and crystallite size was confirmed from XRD data and Fig. 1D shows the X-Ray Diffraction pattern. XRD pattern shows three main reflections (111), (200), (220), (311), (222), and (440) as characteristic of cerium oxide cubic phase with fluorite structure. The calculated lattice parameters was 5.404 Å.

Broad peaks of reflection were clearly visible, indicating small crystal size, and nanoscale dimension, thus proving the success of the proposed method. The phases found were indexed, after analysis and correlation, using the JCPDS 34-0394 datasheet (Joint Committee on Powder Diffraction Standards) for the structure, fluorite, CeO₂.

Fig. 1E was obtained by means of energy dispersive spectroscopy, and it confirm the presence of cerium in the CeNP.

The wavelength at which the maximum absorbance occurs around 300 nm (Fig. 1F).

The average zeta potential for CeNP was from -12.6 ± 0.3 mV.

3.2. Minimum inhibitory concentration and minimum fungicidal concentration

CeNP was able to inhibit the growth of all *Candida* strains tested. *C. albicans* LM 65 and ATCC 76485 strains showed the lowest concentration of MIC (1.50 mg/mL). Miconazole Nitrate (concentration ≤ 62 µg/mL) was able to inhibit all strains (Table 1).

3.3. Growth kinetic study

The growth kinetics study was conducted on three strains of *C. albicans* (ATCC 1106, ATCC 76 485, and LM 38) randomly selected in the presence of CeNP with three concentrations

(MIC ÷ 2, MIC, and MICx2) at 1, 4, 8, and 10 h. In the figure, it is clear that MICx2 had significant effect on strains growth (Fig. 2). At 10 h, CeNP reduced growth of the three strains. For ATCC 1106 (MIC), the survival yeast was 46.35% (Additional file – Fig. S2A). For ATCC 76,485 (MIC), the survival yeast was 49.8% (Additional file – Fig. S2B). LM 38 exposed by CeNP MIC has 59.33% of survival cells (Additional file – Fig. S2C). At 10 h, the highest inhibition of yeast growth was observed at a concentration of 15.0 mg/mL (MICx2) in the ATCC 1106 strain.

3.4. Analysis of the substrate pH

The results showed higher pH with increasing CeNP in the suspension containing the fungus and the culture medium. The pH of the SDB + fungi + CeNP suspension was 10.0, higher than the pH of the SDB + fungi solution (pH 5.0). The SDB + CeNP suspension had a pH of 7.0.

3.5. DPPH radical scavenging activity

The results showed that CeNP showed an average antioxidant activity of $15.06 \pm 0.78\%$ (Fig. 2D). Ascorbic acid at a concentration of 9.23 ± 0.29 µg/mL exhibited a percentage inhibition of 50% and for 18 µg/mL 100%.

3.6. Acute oral toxicity study on mice

No behavioral changes were observed during the study. One death was recorded in the first group treated with 2000 mg/kg of CeNP.

3.6.1. Effects on food and water consumption, and body weight

Table 2 contains values related to water and food consumption evaluated at 14 days of treatment with the substance. Food consumption by the treatment group (with 300 mg/kg, and 2000 mg/kg of CeNP) was significantly reduced when compared with the control group. No significant changes were

Table 1 MIC and MFC of the CeNP and Miconazole Nitrate against strains of *C. albicans*.

Strains	CeNP [‡]		Miconazole Nitrate	
	MIC [§] mg/mL	MFC mg/mL	MIC µg/mL	MFC µg/mL
ATCC* 1106	7.50	12.5	35	62
ATCC 26645	3.17	13.8	35	50
ATCC 60193	3.17	13.8	35	50
ATCC 76485	1.50	22.5	15	30
ATCC 76645	3.17	13.8	35	50
LM [†] 38	2.50	22.5	< 5	30
LM 62	3.17	13.8	< 5	50
LM 65	1.50	22.5	15	30
LM 92	1.75	12.5	35	30
LM 157	3.17	13.8	35	50
LM 227	3.17	13.8	35	50

* American Type Culture Collection.

† Laboratory of Microbiology (Clinical strain).

‡ Cerium oxide nanoparticle.

§ Minimum inhibitory concentration.

|| Minimum fungicidal concentration.

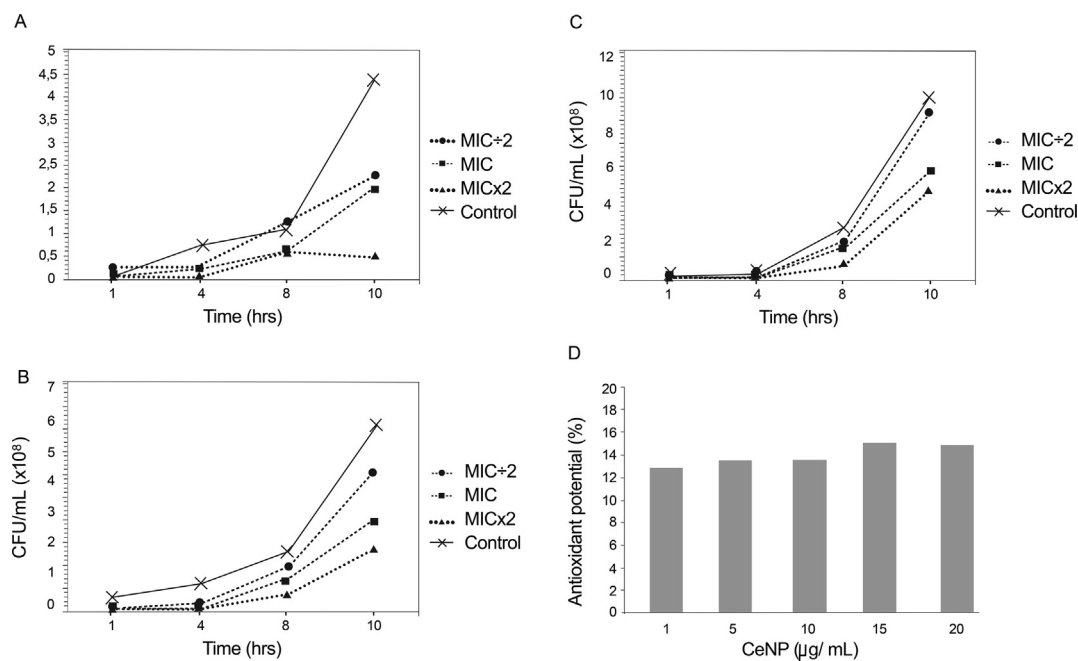


Fig. 2 Growth kinetics of the strain *Candida albicans* in the presence of MIC ÷ 2, MIC, and MICx2 of CeNP. Ten hour growth curve showing the sensitivity of (A) ATCC 1106 to CeNP at 3.75 mg/mL (MIC ÷ 2), 7.5 mg/mL (MIC), and at 15.0 mg/mL (MICx2); (B) ATCC 76485 to CeNP 0.75 mg/mL (MIC ÷ 2), 1.50 mg/mL (MIC) and 3.0 mg/ml (MICx2); and (C) LM 38 to CeNP at 1.25 (MIC ÷ 2), 2.50 mg/mL (MIC), and 5.0 mg/ml (MICx2). In each case, the growth of the strain is control. Note different scales. (D) DPPH radical scavenging potential of CeNP remained low and constant regardless of the concentration of nanoparticles in the acellular system for 90 min of contact between CeNP e DPPH.

Table 2 Food and water consumption, assessed daily, and weight evaluation of animals subjected to treatment with CeNP.

Groups	Dose mg/kg	Water consumption mL	Food consumption g	Initial weight g	Final weight g
Control	–	48.8 ± 2.7	58.9 ± 3.2	31.5 ± 0.8	35.4 ± 0.7
CeNP*	300	40.9 ± 2.7	44.6 ± 3.0 [†]	30.6 ± 0.7	34.6 ± 1.5
CeNP	2000	52.3 ± 5.0	42.0 ± 4.4 [†]	31.0 ± 0.9	34.1 ± 0.3

Data presented as mean ± standard error of the mean of 5–6 animals analyzed by ANOVA with Tukey post test.

[†] $p < 0.05$ compared to control.

* Cerium oxide nanoparticle.

Table 3 Effect of CeNP in biochemical parameters in peripheral blood of mice.

Groups	Dose mg/kg	AST [†] U/L	ALT [‡] U/L	Urea mg/dL	Creatinine mg/dL
Control	–	137.4 ± 13.8	61.9 ± 5.0	38.7 ± 4.8	0.4 ± 0.07
CeNP*	300	165.5 ± 62.1	46.0 ± 24.8	31.1 ± 2.0	0.3 ± 0.01
CeNP	2000	128.8 ± 18.7	52.6 ± 6.5	60.6 ± 9.3 ^{§,}	0.4 ± 0.06

Data presented as mean ± standard error of the mean of 5–6 animals analyzed by ANOVA with Tukey post test.

[§] $p < 0.05$ compared to control.

^{||} $p < 0.05$ compared to 300 mg/kg.

* Cerium oxide nanoparticle.

[†] Aspartate aminotransferase

[‡] Alanine aminotransferase

observed in water consumption or weight of the animals after treatment with CeNP, when compared to the control group.

3.6.2. Hematology and biochemical evaluation

As shown in Table 3, there were no significant differences in the AST, ALT, and creatinine parameters between control and treatment groups. However we observed a significant increase of urea in the mice treated with 2000 mg/kg of CeNP, when compared with the control group.

Regarding the hematological evaluation, CeNP did not significantly affect a majority of the hematological parameters of the animals treated. A significant increase in the red blood cell counts of the animals treated with 2000 mg/kg of CeNP was observed. We also observed a significant increase in monocyte counts for the groups treated with CeNP at 300 mg/kg, and 2000 mg/kg (Table 4).

3.6.3. Effects on relative organ weights

Treatment with the substance under study did not result in significant changes in kidney, heart, spleen, and thymus indexes (Table 5). However, a significant increase in the liver index of animals treated with the highest dose of CeNP was observed (Table 5).

3.6.4. Histopathology findings

Histopathological analyses of liver of control and treated groups showed normal histological architecture without periportal and periseptal activity, and fibrosis (Fig. 3). At 300 mg/kg of CeNP, it was observed discreet portoparenchymatous inflammatory processes, and rare foci of hepatocellular necrosis. At 2000 mg/kg, the livers of the animals treated with CeNP also presented portoparenchymatous inflammatory processes with multifocal lobular necrosis, probably of toxic nature, and multifocal sub-capsular granulomatous inflammatory

processes with the absence of cellular atypia (Fig. 3). The changes observed are described in Table 6.

Histopathological analyses of kidneys of control and 300 mg/kg CeNP groups showed normal histology. At 2000 mg/kg of CeNP, it was observed focal interstitial nephritis and necrosis of proximal tubular epithelium (Fig. 3).

3.7. Acute toxicity against *Artemia salina*

The cytotoxicity assay in the *Artemia salina* animal model did not reveal a LD50 or LC50 (lethal dose or minimum lethal concentration of 50%). Exposure to CeNP did not cause death to the naupli in concentrations of 0.001 up to 15.0 mg/mL. The mortality in the group exposed to concentrations of 20.0 and 25.0 mg/mL of CeNP was 4 and 10%, respectively, demonstrating the non-toxicity of CeNP against *A. salina*.

4. Discussion

From the viewpoint of using CeNP in nanostructure engineering with biomedical applications, the synthesis route presented in this study revealed a product with pure phases and with a linear format and thin nanometric layers overlapping for different characterization techniques. The interplanar distances are of the lowest energy level (Deus et al., 2013).

Microwave-mediated synthesis has the advantage of rapid volumetric heating, energy shaving, high-efficiency, economy, high purity and yields over the other conventional method of synthesis (Soren et al., 2015; Goharshadi et al., 2011).

This hydrothermal reaction led to smaller particles ~ 4 nm. This particle size is similar of the other studies than used similar rote of synthesis (Hardas et al., 2012; Goharshadi et al., 2011). However, CeNP with upper crystalline size has been synthesized by autoclave-mediated hydrothermal (Shajahan et al., 2020) as well as microwave-mediated hydrothermal synthesis (Soren et al., 2015).

CeNP with different sizes and characteristics can be obtained by hydrothermal method and by using different precursors agents such as cerium sulfate (used in this study), cerium nitrate (Shajahan et al., 2020; Babu et al., 2014; Krishnamoorthy et al., 2014; Celardo et al., 2011; Goharshadi et al., 2011), and ceric ammonium nitrate (Soren et al., 2015).

The CeNPs surface area observed in this study were two-fold higher than of previous nanoparticle studies (Yokel et al., 2013; Hardas et al., 2012; Celardo et al., 2011), but lower than another study (Zeyons et al., 2009). Thus, the small size of the CeNPs of this study is within previous reported values and it could be confirmed by TEM images and also confirmed by BET surface area. The size of nanoparticles is inversely proportional to the active surface area, and provided a large surface potential for catalysis (Soren et al., 2015; Yokel et al., 2013).

These small particles was tested against eleven strains of *C. albicans*. The nanometric thickness permitted inhibition of *C. albicans* (Babenco et al., 2012). The particle size also allows greater interaction between the nanoparticle and the fungal cell. It can be suggested that at this size metal passes through the barriers which increases interaction between the nanoparticle and pathogen at the cell membrane level (Raghupathi et al., 2011; Zeyons et al., 2009).

Table 4 Effect of CeNP in hematological parameters of peripheral blood of mice.

Parameters	Control	CeNP* 300 mg/kg	CeNP 2000 mg/kg
Red blood cells ($10^6/\text{mm}^3$)	8.8 ± 0.1	7.3 ± 0.5	10.0 ± 0.2
Hemoglobin (g/dL)	13.3 ± 0.3	13.0 ± 0.5	14.2 ± 0.5
Hematocrit (%)	50.6 ± 1.6	53.3 ± 1.9	54.0 ± 1.8
MCV [†] (fm ³)	57.4 ± 1.4	59.8 ± 1.6	54.2 ± 1.7
MCH [‡] (pg)	15.1 ± 0.4	14.7 ± 0.5	14.2 ± 0.4
MCHC [§] (g/dL)	26.5 ± 0.9	24.8 ± 1.3	26.3 ± 0.7
Leukocytes ($10^3/\text{mm}^3$)	4.1 ± 0.7	2.5 ± 0.5	2.8 ± 0.2
Lymphocytes	66.7 ± 3.7	69.5 ± 2.3	59.4 ± 4.9
Neutrophils	28.6 ± 3.3	24.8 ± 1.3	33.2 ± 4.8
Monocytes	4.4 ± 0.6	7.3 ± 0.5	7.4 ± 1.4
Eosinophils	1.3 ± 0.3	1.0 ± 0.0	0.0 ± 0.0

Data presented as mean ± standard error of the mean of 5–6 animals analyzed by ANOVA with Tukey post test.

^{||} $p < 0.05$ compared to control.

* Cerium oxide nanoparticle.

[†] Mean corpuscular volume.

[‡] Mean corpuscular haemoglobin.

[§] Mean corpuscular hemoglobin concentration.

Table 5 Effect of CeNP in the indexes of the organs of mice.

Groups	Dose mg/kg	Index of thymus mg/g	Index of spleen mg/g	Index of liver mg/g	Index of kidneys mg/g	Index of heart mg/g
Control	–	4.1 ± 0.4	5.8 ± 0.3	64.8 ± 1.7	12.3 ± 0.4	4.5 ± 0.1
CeNP*	300	4.1 ± 0.3	6.1 ± 0.5	63.2 ± 2.3	12.0 ± 0.5	4.3 ± 0.1
CeNP	2000	5.0 ± 0.6	6.0 ± 0.8	73.7 ± 2.1 ^{†,‡}	13.8 ± 0.9	4.8 ± 0.2

Data presented as mean ± standard error of the mean of 5–6 animals analyzed by ANOVA with Tukey post test.

[†] $p < 0.05$ compared to control.

[‡] $p < 0.05$ compared to 300 mg/kg.

* Cerium oxide nanoparticle.

ATCC and clinical strains were assayed for differing sensibilities of the yeast species involved in fungal infections (Mohr et al., 2020; Zhan et al., 2015; Lim et al., 2012). Strains were standardized (1×10^6 CFU/mL) to prevent inhibitory concentration variation because of differences in the amount of fungus (Lara et al., 2015). The therapeutic concentration of CeNPs fungal inhibition was from 1.50 to 22.5 mg/mL, considering the small difference in MIC and MFC values among strains. These values show that CeNP was ~ 100-fold less potent than miconazole nitrate. A similar concentration of CeNP (1.72 mg/mL) was found in one study that addresses antifungal activity (Babenko et al., 2012) and silver-zinc oxide nanoparticles (Burlibaşa et al., 2020).

The CeNP presented antifungal activity proportional to increased concentrations, however, lower minimum inhibitory concentrations were observed in silver and zinc particles nanoparticles (Artunduaga Bonilla et al., 2015; Lara et al., 2015; Shoeb et al., 2013) probably due to the tendency of crystallites of cerium oxide to form agglomerates under the influence of Van der Waals forces or strong chemical bonds between individual particles (Rubio et al., 2016). It is suggested that the agglomerates impair fungal specific bioactivity by reducing the contact between nanoparticles and the cell through reduced contact surface area (Celardo et al., 2011).

CeNP in medium containing *C. albicans* increased the pH; resulting in an unfavorable environment for fungus growth (Lim et al., 2012). However, it was observed (Zeyons et al., 2009) that CeNP in ultrapure water in contact with cyanobacteria reduces the pH, resulting in an unfavorable environment for microorganisms (indirect effect). The direct effect occurs due to the contact between CeNP and bacteria like *E. coli* (Zeyons et al., 2009).

UV – VIS absorption spectra of CeNPs with maximum absorption at 300 nm, indicative of (4f⁰) Ce⁴⁺. The mechanism of CeNP action likely occurs through oxidative stress. In the direct contact between nanoparticle and the outer microorganism membrane occur alteration in nanoparticle and microorganism surface. Ce⁴⁺ is converted Ce³⁺ with oxidation of the lipid membrane/ proteins or capture of electrons from metabolic processes (Zeyons et al., 2009). Oxi-reduction reaction is probably favored by increase of environment pH (Farias et al., 2018).

The active role of microorganism in the reduction of Ce⁴⁺ is indisputable (Zeyons et al., 2009). In relation pH is not different: this present study shows the alkaline medium was not observed in abiotic medium.

Environmental alkaline pH was observed in medium + CeNP + fungi. By contrast, environment pH acidic was observed in the medium with *Candida albicans*, without nanoparticles. Environmental acid is favorable for biofilm formation (cell counts and metabolic activity) (Vasconcellos et al., 2014). Probably, the pH increase is influenced by contact between fungi and CeNP and, therefore, alkaline pH is a consequence of CeNP activity against *Candida albicans*.

Toxicological screening is very important for the development of new drugs and for the extension of the therapeutic potential of existing molecules. In acute toxicological testing, the investigational product is administered at different dose levels, and the effect is observed for 14 days. Following dosing, the animals are monitored for overt toxicological signs until death (Parasuraman, 2011). The acute toxicity test used here (Acute Toxic Class method - OECD 423; OECD, 2001) permits to estimate the LD50 (median lethal oral dose) and to classify the substance using the Globally Harmonized Classification System for Chemical Substances and Mixtures (GHS). The results showed that the LD50 value is greater than 2000 mg/kg and CeNP was ranked into category 5 of GHS (OECD, 2001).

The outcomes on the food consumption have demonstrated that significative reduction with treatment with CeNP. The increase of urea observed suggests renal function interference, which also can be considered to be of little clinical importance, since no significant changes were observed in serum creatinine.

Despite the increase of red blood cells counts, they were within normal parameters for mice ($9\text{--}11.5 \times 10^6$ cells/mm³) (Hall, 2007). Regarding alterations observed in the monocyte count, they might be explained by the fact that the primary function of the monocytes is phagocytosis and digestion of large particulate matter, the increase of this cell type in the groups treated with 300 mg/kg and 2000 mg/kg of CeNP, could be a reaction to the nanoparticles. With respect to the organ indexes, a significant increase in the liver indexes of the mice treated with 2000 mg/kg of CeNP was evidenced, a possible indication of subcellular changes. Organs weights are frequently the earliest indicator of affected organs (Hall, 2007).

Regarding to histopathological analysis, the results showed inflammatory processes as a consequence of toxic aggressions at 2000 mg/kg of CeNP. Recent data showed that a single dose of 2000 mg/kg of CeNPs induced tissue damage and focal areas of necrosis (Kumari et al., 2014). Previous study reported that that CeNP administered a single dose of 0.5 mg/kg body weight did not revealed any impairment of the tissues (Rocca

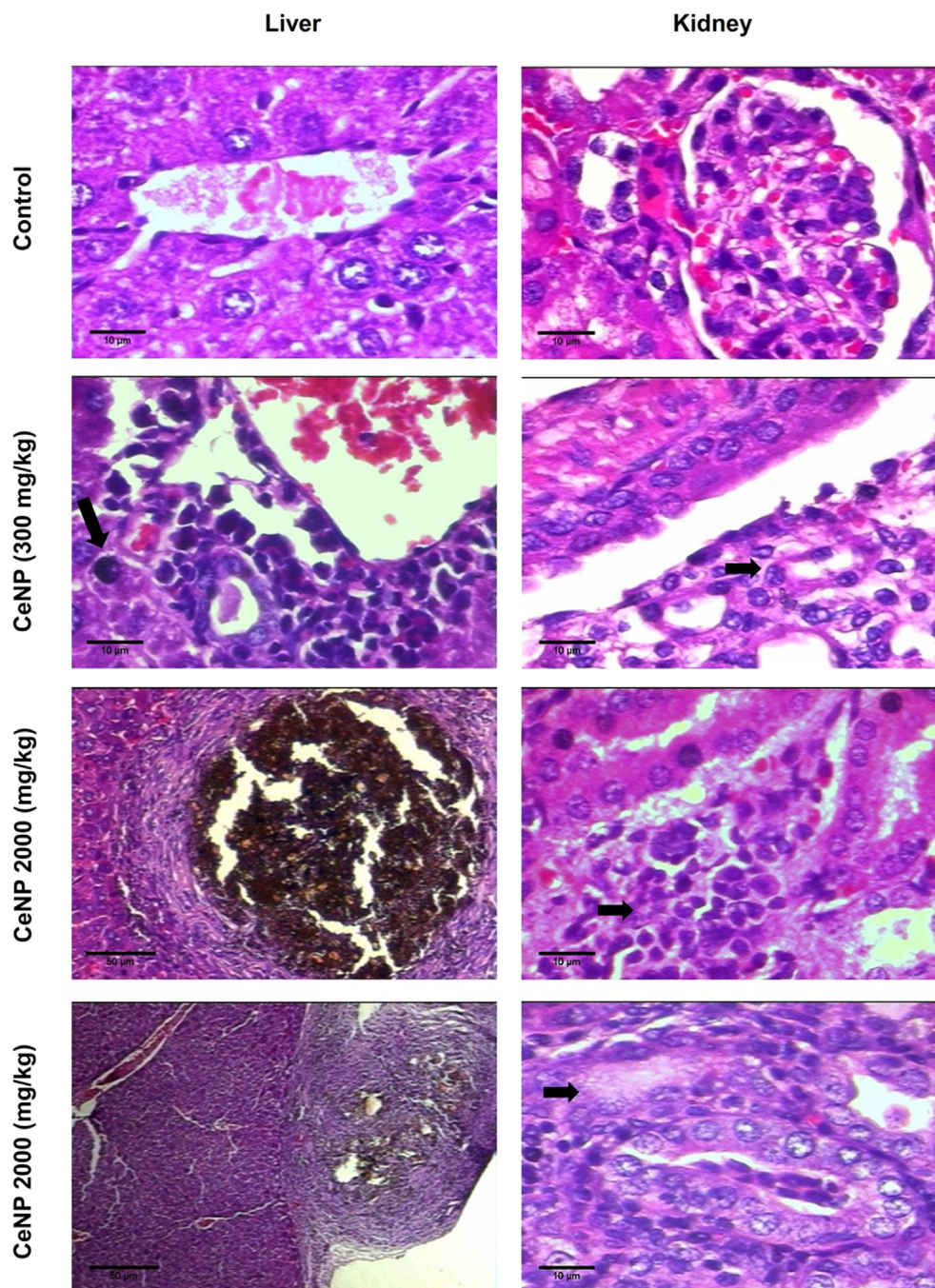


Fig. 3 Histopathology analysis - the liver was examined: Control - Normal hepatocytes, isomorphic; CeNP (300 mg/kg) group - presence of inflammatory infiltrate around the lobular vein and rare foci of hepatocellular necrosis (arrows point); CeNP (2000 mg/kg) group - multifocal sub-capsular granulomatous inflammatory processes. Histopathology analysis - the kidneys were examined: Control - Glomerulus preserved with thin Bowman's capsule, capillary tuft supported by delicate mesangium; CeNP (300 mg/kg) group - Distal convoluted tubule normal, and discreet increase in the number of portal lymphocytes, along with some polymorphonuclear neutrophils in rare portal spaces (arrows point); CeNP (2000 mg/kg) group - focal interstitial nephritis (arrows point). Hematoxylin-Eosin. All the images were 400× the original magnification.

et al., 2015). However, liver effect may be due to the fact that it is the first organ to be exposed to NPs after entry into the circulation system because of its major role in biotransformation of toxins and foreign materials (Kumari et al., 2014), and the high dose of CeNP gets in the way nanoparticle clearance (Rocca et al., 2015).

In addition, we have not observed marked changes, such as steatosis and fibrosis, after treatment with CeNP. The histopathological findings for both doses of CeNP are reported in the literature as weak evidence of toxicity; in which withdrawing the drug, or adjusting the dose usually leads to a rapid improvement and/or reversal of damage (Montenegro et al.,

Table 6 Effect of CeNP (300 or 2000 mg/kg) on histopathology changes in liver tissue of mice after a single dose of oral treatment.

Parameters	Groups	Histopathology changes	Score
Portal inflammatory infiltrate	Control	Normal histopathology	0
	300 mg/kg CeNP*	Discreet increase in the number of portal lymphocytes, along with some polymorphonuclear neutrophils in rare portal spaces	1
	2000 mg/kg CeNP	Moderate increase in the number of portal lymphocytes, along with polymorphonuclear neutrophils in some portal spaces	2
Parenchymal activity	Control	Normal histopathology	0
	300 mg/kg CeNP	Discreet hepatocytic alterations with lymphohistiocytic infiltrate and rare necrotic areas. The parenchymal necrosis foci are seen randomly in zones I, II and III	1
	2000 mg/kg CeNP	Focal hepatocyte necrosis surrounded by lymphohistiocytic aggregate. The parenchymal necrosis foci are seen randomly in zones I, II and III	2

* Cerium oxide nanoparticle.

2008; Vasconcellos et al., 2007). Moreover, these findings should not be relevant to humans, considering that very high doses were used. This result, associated with the absence of significant changes in most of the parameters analyzed, suggest low acute toxicity.

Besides the mice model, the data show the *A. salina* toxicity evaluation. This organism is the standard for research on nanoparticles (Ozkan et al., 2016; Rajabi et al., 2015; Ates et al., 2013; Radhika Rajasree et al., 2010).

A. salina exposure to CeNP up to a concentration of 15.0 mg/mL CeNP did not induce any significant lethal effects, disagreeing with a previous study that observed inhibition of swimming in larvae exposed to 0.1 and 1.0 mg/mL CeNP (Gambardella et al., 2014).

It is important to point out that the CeNP concentrations tested in the toxicological screening were lower than the inhibitory concentration, minimum fungicidal. The pH measured before the count showed an optimum and stable pH. Probably the reason for mortality was the formation of aggregates and accumulations of CeNP inside *A. salina*, not excreted (Gambardella et al., 2014; Ates et al., 2013).

DPPH free radical scavenging potential of CeNP remained low and constant regardless of the concentration of nanoparticles. Similar data were observed previously using a sediment fraction of CeNP (Celardo et al., 2011). Nanoparticles synthesized in this study presented maximum absorbance in the

valence state Ce^{4+} , suggesting Ce^{4+} to Ce^{3+} reaction and characterizing nanoparticles with pro-oxidative activity (Soren et al., 2015; Hardas et al., 2012; Hirst et al., 2009; Zeyons et al., 2009).

However, the antioxidant activity of cerium oxide nanoparticles was observed in a previous study using free radical (DPPH), being evidenced significant inhibition of free radicals by small concentrations of CeNP (Soren et al., 2015). It is important to note that the assessment used in this study differs from others (Soren et al., 2015; Celardo et al., 2011), for having used a mainly cell-free system. Furthermore, the agglomeration of the crystallites increases in number and size with increasing CeNP concentration in colloidal aqueous dispersion (Celardo et al., 2011), suggesting decreases in the available contact surface with the DPPH radical. The antioxidant activity of CeNP has been explored at several biologic application: radioprotective effects on stem cells (Salvetti et al., 2020), neuroprotective and pro-neurogenic agent with nanoparticle into a lipid-based delivery system (Battaglini et al., 2019), potential pharmaceutical approach for the treatment of neurodegenerative diseases (Battaglini et al., 2019), diseases caused by oxidative stresses, including those related with pulmonary system (Rubio et al., 2016), and of obesity (Rocca et al., 2015).

However, CeNP synthesized in the present study by the microwave-hydrothermal method with the use of cerium sulfate as the precursor salt result nanoparticles antifungal activities, toxicity no relevant (toxicity at high doses), but low antioxidant activity.

5. Conclusions

The current antifungal and toxicity features results support the use of CeNP as antifungal agent against *Candida albicans* strains, which may find applications in biotechnology and biomedical area in the development of a new nanobiomaterial for clinical applications.

Declaration of Competing Interest

The authors declare that they have no known competing financial interests or personal relationships that could have appeared to influence the work reported in this paper.

Acknowledgements

We would like to thanks to Centro de Tecnologias Estratégicas do Nordeste (CETENE/ Pernambuco/ Brazil) for the TEM images.

Author Contributions

All authors have made essential contributions to this study. Experimental design: I.A.P.F., C.L.S. and F.C.S. Nanoparticle synthesis and characterization: C.L.S, J.M.F and D.K. Biological experiments: I.A.P.F., J.M.F.F.N., A.L.X, T.M.B., P.M. F.S., R.A.M.J, E.O.L., M.V.S., F.C.S. G.P.R. and I.R.P. Antioxidant activity experiment: I.A.P.F, T.M.B, Y.M.N., J. F.T., M.V.S. and F.C.S. Manuscript drafting: I.A.P.F., A.L. X., M.V.S. and F.C.S. All authors read and approved the final manuscript.

Funding

This manuscript was supported by the Coordenação de Aperfeiçoamento de Pessoal de Nível Superior (CAPES; www.capes.gov.br) and Conselho Nacional de Desenvolvimento Científico e Tecnológico (CNPq; www.cnpq.br).

Ethics approval

Experimental protocols and procedures were approved by the local animal ethics committee (protocol number 016/2016) which follows the international principles in ethics for animal experimentation.

Appendix A. Supplementary material

Supplementary data to this article can be found online at <https://doi.org/10.1016/j.arabjc.2020.10.035>.

References

- Almeida, R.N., Falcão, A.C.G.M., Diniz, R.S.T., Almeida, R.N., Falcão, A.C.G.M., Diniz, R.S.T., Quintans-Júnior, L.J., Polari, R. M., Barbosa Filho, J.M., Agra, M.F., Duarte, J.C., Ferreira, C.D., Antonioli, A.R., Araújo, C.C., 1999. Methodology for evaluation of plants with central nervous system and some experimental data. *Rev. Bras. Farm.* 80, 72–76.
- Artunduaga Bonilla, J.J., Paredes Guerrero, D.J., Sánchez Suárez, C. I., Ortiz López, C.C., Torres Sáez, R.G., 2015. *In vitro* antifungal activity of silver nanoparticles against fluconazole-resistant *Candida* species. *World J. Microbiol. Biotechnol.* 31, 1801–1809. <https://doi.org/10.1007/s11274-015-1933-z>.
- Ates, M., Daniels, J., Arslan, Z., Farah, I.O., Rivera, H.F., 2013. Comparative evaluation of impact of Zn and ZnO nanoparticles on brine shrimp (*Artemia salina*) larvae: effects of particle size and solubility on toxicity. *Environ. Sci. Process. Impacts.* 15, 225–233. <https://doi.org/10.1039/c2em30540b>.
- Babenko, L.P., Zholobak, N.M., Shcherbakov, A.B., Voychuk, S.I., Lazarenko, L.M., Spivak, M.Y., 2012. Antibacterial activity of cerium colloids against opportunistic microorganisms *in vitro*. *Mikrobiol Z.* 74, 54–62.
- Babu, K.S., Anandkumar, M., Tsai, T.Y., Kao, T.H., Inbaraj, B.S., Chen, B.H., 2014. Cytotoxicity and antibacterial activity of gold-supported cerium oxide nanoparticles. *Int. J. Nanomed.* 27, 5515–5531. <https://doi.org/10.2147/IJN.S70087>.
- Battaglini, M., Tapeinos, C., Cavaliere, I., Marino, A., Ancona, A., Garino, N., Cauda, V., Palazon, F., Debellis, D., Ciofani, G., 2019. Design, fabrication, and *in vitro* evaluation of nanoceria-loaded nanostructured lipid carriers for the treatment of neurological diseases. *ACS Biomater. Sci. Eng.* 5, 670–682. <https://doi.org/10.1021/acsbomaterials.8b01033>.
- Brunauer, S., Emmett, P.H., Teller, E., 1938. Adsorption of gases in multimolecular layers. *J. Am. Chem. Soc.* 60, 309–319. <https://doi.org/10.1021/ja01269a023>.
- Brunt, E.M., Janney, C.G., Di Bisceglie, A.M., Neuschwander-Tetri, B.A., Bacon, B.R., 1999. Nonalcoholic steatohepatitis: a proposal for grading and staging the histological lesions. *Am. J. Gastroenterol.* 94, 2467–2474. <https://doi.org/10.1111/j.1572-0241.1999.01377.x>.
- Burlibaşa, I., Chifriuc, M.C., Lungu, M.V., Lungulescu, E.M., Mitrea, S., Sbarcea, G., Popa, M., Măruţescu, L., Constantin, N., Bleotu, C., Hermenean, A., 2020. Synthesis, physico-chemical characterization, antimicrobial activity and toxicological features of AgZnO nanoparticles. *Arab. J. Chem.* 13, 4180–4197. <https://doi.org/10.1016/j.arabjc.2019.06.015>.
- Montenegro, R.C., Feio Farias, R.A., Pinho Pereira, M.R., Negreiros Nunes Alves, A.P., Silva Bezerra, F., Andrade-Neto, M., Pessoa, C., de Moraes, M.O., Veras Costa-Lotuf, L., 2008. Antitumor activity of pisolsterol in mice bearing with S180 tumor. *Biol. Pharm. Bull.* 31, 454–457. <https://doi.org/10.1248/bpb.31.454>.
- Celardo, I., De Nicola, M., Mandoli, C., Pedersen, J.Z., Traversa, E., Ghibelli, L., 2011. Ce³⁺ ions determine redox-dependent anti-apoptotic effect of cerium oxide nanoparticles. *ACS Nano.* 5, 4537–4549. <https://doi.org/10.1021/nn200126a>.
- Chigurupati, S., Mughal, M.R., Okun, E., Das, S., Kumar, A., McCaffery, M., Seal, S., Mattson, M.P., 2013. Effects of cerium oxide nanoparticles on the growth of keratinocytes, fibroblasts and vascular endothelial cells in cutaneous wound healing. *Biomaterials.* 34, 2194–2201. <https://doi.org/10.1016/j.biomaterials.2012.11.061>.
- Deus, R.C., Cilense, M., Foschini, C.R., Ramirez, M.A., Longo, E., Simões, A.Z., 2013. Influence of mineralizer agents on the growth of crystalline CeO₂ nanospheres by the microwave-hydrothermal method. *J. Alloy. Compd.* 550, 245–251. <https://doi.org/10.1016/j.jallcom.2012.10.001>.
- EPA, United States Environmental Protection Agency, 2002. Methods for measuring the acute toxicity of effluents and receiving waters to freshwater and marine organisms. EPA 821-R-02-012. https://www.epa.gov/sites/production/files/2015-08/documents/acute-freshwater-and-marine-wet-manual_2002.pdf (accessed 07 October 2020).
- Farias, I., Santos, C., Sampaio, F.C., 2018. Antimicrobial activity of cerium oxide nanoparticles on opportunistic microorganisms: a systematic review. *BioMed Res. Int.* 2018, 1923606. <https://doi.org/10.1155/2018/1923606>.
- Fekkar, A., Dannaoui, E., Meyer, I., Imbert, S., Brossas, J.Y., Uzunov, M., Mellon, G., Nguyen, S., Guiller, E., Caumes, E., Leblond, V., Mazier, D., Fievet, M.H., Datry, A., 2014. Emergence of echinocandin-resistant *Candida* spp. in a hospital setting: a consequence of 10 years of increasing use of antifungal therapy?. *Eur. J. Clin. Microbiol. Infect. Dis.* 33, 1486–1496. <https://doi.org/10.1007/s10096-014-2096-9>.
- Gambardella, C., Mesarič, T., Milivojević, T., Sepčić, K., Gallus, L., Carbone, S., Ferrando, S., Faimali, M., 2014. Effects of selected metal oxide nanoparticles on *Artemia salina* larvae: evaluation of mortality and behavioural and biochemical responses. *Environ. Monit. Assess.* 186, 4249–4259. <https://doi.org/10.1007/s10661-014-3695-8>.
- Goharshadi, E.K., Samiee, S., Nancarrow, P., 2011. Fabrication of cerium oxide nanoparticles: characterization and optical properties. *J. Colloid. Interface Sci.* 356, 473–480. <https://doi.org/10.1016/j.jcis.2011.01.063>.
- Hall, R.L., 2007. Clinical pathology of laboratory animals in Animal models in toxicology. In: Gad, S.C., Animal Models in Toxicology. CRC Press, New York, pp. 787–830.
- Hardas, S.S., Sultana, R., Warriar, G., Dan, M., Florence, R.L., Wu, P., Grulke, E.A., Tseng, M.T., Unrine, J.M., Graham, U.M., Yokel, R.A., Butterfield, D.A., 2012. Rat brain pro-oxidant effects of peripherally administered 5 nm ceria 30 days after exposure. *Neurotoxicology.* 33, 1147–1155. <https://doi.org/10.1016/j.neuro.2012.06.007>.
- Hirst, S.M., Karakoti, A.S., Tyler, R.D., Sriranganathan, N., Seal, S., Reilly, C.M., 2009. Anti-inflammatory properties of cerium oxide nanoparticles. *Small.* 5, 2848–2856. <https://doi.org/10.1002/sml.200901048>.
- Jin, Y., Zhang, T., Samaranayake, Y.H., Fang, H.H.P., Yip, H.K., Samaranayake, L.P., 2005. The use of new probes and stains for improved assessment of cell viability and extracellular polymeric substances in *Candida albicans* biofilms. *Mycopathologia.* 159 (3), 353–360. <https://doi.org/10.1007/s11046-004-6987-7>.

- Khan, I., Saeed, K., Khan, I., 2019. Nanoparticles: Properties, applications and toxicities. *Arab. J. Chem.* 12, 908–931. <https://doi.org/10.1016/j.arabjc.2017.05.011>.
- Koehler, P., Stecher, M., Cornely, O., Koehler, D., Vehreschild, M.J.G.T., Bohlius, J., Wisplinghoff, H., Vehreschild, J.J., 2019. Morbidity and mortality of candidaemia in Europe: an epidemiologic meta-analysis. *Clin. Microbiol. Infect.* 25, 1200–1212. <https://doi.org/10.1016/j.cmi.2019.04.024>.
- Krishnamoorthy, K., Veerapandian, M., Zhang, L.H., Yun, K., Kim, S.J., 2014. Surface chemistry of cerium oxide nanocubes: toxicity against pathogenic bacteria and their mechanistic study. *J. Ind. Eng. Chem.* 20, 3513–3517. <https://doi.org/10.1016/j.jiec.2013.12.043>.
- Kumari, M., Kumari, S.I., Kamal, S.S.K., Grover, P., 2014. Genotoxicity assessment of cerium oxide nanoparticles in female Wistar rats after acute oral exposure. *Mutat. Res. Genet. Toxicol. Environ. Mutagen.* 775–776, 7–19. <https://doi.org/10.1016/j.mrgentox.2014.09.009>.
- Lara, H.H., Romero-Urbina, D.G., Pierce, C., Lopez-Ribot, J.L., Arellano-Jiménez, M.J., Jose-Yacamán, M., 2015. Effect of silver nanoparticles on *Candida albicans* biofilms: an ultrastructural study. *J. Nanobiotechnol.* 13, 91. <https://doi.org/10.1186/s12951-015-0147-8>.
- Lim, C.S., Rosli, R., Seow, H.F., Chong, P.P., 2012. Candida and invasive candidiasis: back to basics. *Eur. J. Clin. Microbiol. Infect. Dis.* 31, 21–31. <https://doi.org/10.1007/s10096-011-1273-3>.
- Mauro, M., Crosera, M., Monai, M., Montini, T., Fornasiero, P., Bovenzi, M., Adami, G., Turco, G., Filon, F.L., 2019. Cerium oxide nanoparticles absorption through intact and damaged human skin. *Molecules* 24 (20), 3759. <https://doi.org/10.3390/molecules24203759>.
- Medeiros, P.J., Villarim Neto, A., Lima, F.P., Azevedo, I.M., Leão, L.R.S., Medeiros, A.C., 2010. Effect of sildenafil in renal ischemia/reperfusion injury in rats. *Acta Cir. Bras.* 25, 490–495. <https://doi.org/10.1590/s0102-86502010000600006>.
- Melchionna, M., Fornasiero, P., 2014. The role of ceria-based nanostructured materials in energy applications. *Mat. Today.* 17, 349–357. <https://doi.org/10.1016/j.mattod.2014.05.005>.
- Mohr, A., Simon, M., Joha, T., Hanses, F., Salzberger, B., Hitzentbichler, F., 2020. Epidemiology of candidemia and impact of infectious disease consultation on survival and care. *Infection.* 48, 275–284. <https://doi.org/10.1007/s15010-020-01393-9>.
- Montini, T., Melchionna, M., Monai, M., Fornasiero, P., 2016. Fundamentals and catalytic applications of CeO₂-based materials. *Chem. Rev.* 116, 5987–6041. <https://doi.org/10.1021/acs.chemrev.5b00603>.
- OECD, Organization for Economic Cooperation & Development, 2001. Test guideline N. 423: Acute oral toxicity - Acute toxic class method. Paris: OECD Publishing; 2001. p. 1–14. <https://www.oecd-ilibrary.org/docserver/9789264071001-en.pdf?expires=1602441932&id=id&accname=guest&checksum=7E2512A328B298E58F5444757200D5CD>. (accessed 11 October 2020).
- Ozkan, Y., Altinok, I., Ilhan, H., Sokmen, M., 2016. Determination of TiO₂ and AgTiO₂ nanoparticles in *Artemia salina*: toxicity, morphological changes, uptake and depuration. *Bull. Environ. Contam. Toxicol.* 96, 36–42. <https://doi.org/10.1007/s00128-015-1634-1>.
- Pappas, P.G., Kauffman, C.A., Andes, D.R., Clancy, C.J., Marr, K.A., Ostrosky-Zeichner, L., Reboli, A.C., Schuster, M.G., Vazquez, J.A., Walsh, T.J., Zaoutis, T.E., Sobel, J.D., 2016. Clinical practice guideline for the management of candidiasis: 2016 update by the Infectious Diseases Society of America. *Clin. Infect. Dis.* 62, e1–e50. <https://doi.org/10.1093/cid/civ933>.
- Parasuraman, S., 2011. Toxicological screening. *J. Pharmacol. Pharmacother.* 2, 74–79. <https://doi.org/10.4103/0976-500X.81895>.
- Pelletier, D.A., Suresh, A.K., Holton, G.A., McKeown, C.K., Wang, W., Gu, B., Mortensen, N.P., Allison, D.P., Joy, D.C., Allison, M.R., Brown, S.D., Phelps, T.J., Doktycz, M.J., 2010. Effects of engineered cerium oxide nanoparticles on bacterial growth and viability. *Appl Environ Microbiol.* 76, 7981–7989. <https://doi.org/10.1128/AEM.00650-10>.
- Pujar, M.S., Hunagund, S.M., Barretto, D.A., Desai, V.R., Patil, S., Vootla, S.K., Sidarai, A.H., 2020. Synthesis of cerium-oxide NPs and their surface morphology effect on biological activities. *Bull. Mater. Sci.* 43, 24. <https://doi.org/10.1007/s12034-019-1962-6>.
- Radhika Rajasree, S.R., Ganesh Kumar, V., Stanley Abraham, L., Indabakandan, D., 2010. Studies on the toxicological effects of engineered nanoparticles in environment—a review. *Int. J. Appl. Bioeng* 4, 44–53. <https://doi.org/10.18000/ijabeg.10083>.
- Raghupathi, K.R., Koodali, R.T., Manna, A.C., 2011. Size-dependent bacterial growth inhibition and mechanism of antibacterial activity of zinc oxide nanoparticles. *Langmuir.* 27, 4020–4028. <https://doi.org/10.1021/la104825u>.
- Rajabi, S., Ramazani, A., Hamidi, M., Naji, T., 2015. *Artemia salina* as a model organism in toxicity assessment of nanoparticles. *Daru* 23, 20. <https://doi.org/10.1186/s40199-015-0105-x>.
- Rocca, A., Moscato, S., Ronca, F., Nitti, S., Mattoli, V., Giorgi, M., Ciofani, G., 2015. Pilot *in vivo* investigation of cerium oxide nanoparticles as a novel anti-obesity pharmaceutical formulation. *Nanomedicine* 11, 1725–1734. <https://doi.org/10.1016/j.nano.2015.05.001>.
- Rubio, L., Annangi, B., Vila, L., Hernández, A., Marcos, R., 2016. Antioxidant and anti-genotoxic properties of cerium oxide nanoparticles in a pulmonary-like cell system. *Arch Toxicol.* 90, 269–278. <https://doi.org/10.1007/s00204-015-1468-y>.
- Salveti, A., Gambino, G., Rossi, L., De Pasquale, D., Pucci, C., Linsalata, S., Degl’Innocenti, A., Nitti, S., Prato, M., Ippolito, C., Ciofani, G., 2020. Stem cell and tissue regeneration analysis in low-dose irradiated planarians treated with cerium oxide nanoparticles. *Mater. Sci. Eng. C* 115. <https://doi.org/10.1016/j.msec.2020.111113> 111113.
- Shajahan, S., Arumugam, P., Rajendran, R., Munusamy, A.P., 2020. Optimization and detailed stability study on Pb doped ceria nanocubes for enhanced photodegradation of several anionic and cationic organic pollutants. *Arab. J. Chem.* 13, 1309–1322. <https://doi.org/10.1016/j.arabjc.2017.11.001>.
- Shoeb, M., Singh, B.R., Khan, J.A., Khan, W., Singh, B.N., Singh, H. B., Naqvi, A.H., 2013. ROS-dependent anticandidal activity of zinc oxide nanoparticles synthesized by using egg albumen as a biotemplate. *Adv. Nat. Sci. Nanotechnol.* 4, <https://doi.org/10.1088/2043-6262/4/3/035015> 035015.
- Soren, S., Jena, S.R., Samanta, L., Parhi, P., 2015. Antioxidant potential and toxicity study of the cerium oxide nanoparticles synthesized by microwave-mediated synthesis. *Appl Biochem Biotechnol.* 177, 148–161. <https://doi.org/10.1007/s12010-015-1734-8>.
- Vasconcellos, A.A., Gonçalves, L.M., Del Bel Cury, A.A., Silva, W.J., 2014. Environmental pH influences *Candida albicans* biofilms regarding its structure, virulence and susceptibility to fluconazole. *Microb. Pathog.* 69–70, 39–44. <https://doi.org/10.1016/j.micpath.2014.03.009>.
- Vasconcellos, M.C., Bezerra, D.P., Fonseca, A.M., Pereira, M.R., Lemos, T.L., Pessoa, O.D., Pessoa, C., Moraes, M.O., Alves, A.P., Costa-Lotufo, L.V., 2007. Antitumor activity of biflorin, an o-naphthoquinone isolated from *Capraria biflora*. *Biol. Pharm. Bull.* 30, 1416–1421. <https://doi.org/10.1248/bpb.30.1416>.

- Yokel, R.A., Tseng, M.T., Dan, M., Unrine, J.M., Graham, U.M., Wu, P., Grulke, E.A., 2013. Biodistribution and biopersistence of ceria engineered nanomaterials: size dependence. *Nanomedicine*. 9, 398–407. <https://doi.org/10.1016/j.nano.2012.08.002>.
- Zeyons, O., Thill, A., Chauvat, F., Menguy, N., Cassier-Chauvat, C., Oréar, C., Daraspe, J., Auffan, M., Rose, J., Spalla, O., 2009. Direct and indirect CeO₂ nanoparticles toxicity for *Escherichia coli* and *Synechocystis*. *Nanotoxicology*. 3, 284–295. <https://doi.org/10.3109/17435390903305260>.
- Zhan, L., Zhou, S., Pan, A., Li, J., Liu, B., 2015. Surveillance of antifungal susceptibilities in clinical isolates of candida species at 36 hospitals in China from 2009 to 2013. *Int. J. Infect. Dis.* 33, 1–4. <https://doi.org/10.1016/j.ijid.2014.12.033>.